LAWRENCE
LIVERMORE
NATIONAL
LABORATORY

LLNL-TR-405954

Experimental Validation of Lightning-Induced Electromagnetic (Indirect) Coupling to Short Monopole Antennas

Eric W. Crull, Charles G. Brown Jr., Mike P. Perkins, Mike M. Ong

August 4, 2008

Disclaimer

This work performed under the auspices of the U.S. Department of Energy by Lawrence Livermore National Laboratory under Contract DE-AC52-07NA27344.

Experimental Validation of Lightning-Induced Electromagnetic (Indirect) Coupling to Short Monopole Antennas

Eric W. Crull
Charles G. Brown Jr.
Mike P. Perkins
Mike M. Ong

1.0 Simple Monopole Antenna Circuit Model

Lightning strikes to "Faraday Cages" at the Pantex facility are a matter of concern while devices are in various stages of disassembly. During a lightning strike there exists the potential for energy to be indirectly coupled into detonator cables via EM fields. If the stress (peak voltage or energy) on a detonator is sufficiently high, the unintended initiation of high explosives is a potential consequence. The stress levels are a function of EM environment variables (rise rates of the lightning current, attachment point, and the quality of the Faraday cages) and coupling issues (location, length, and orientation of the component wires). We use simple circuit models, validated experimentally, to estimate the stress level. For a more in-depth introduction, see Section 5.0.

During a lightning strike, the rebar in the Faraday cage structure conducts current, which creates electric and magnetic fields within the cell. Since the cell is electrically small (its dimensions are much less than the smallest wavelength of interest), a simple quasi-static approximation of the fields within can be invoked. Accordingly, the magnetic field is proportional to the lightning current; the electric field is proportional to the first derivative of the lightning current (see [1]). In this report we will assume we are given the time-varying, worst-case electric and magnetic fields as

$$B(t) = \frac{B_{\max}}{I_{\max}} I(t)$$

$$E(t) = \frac{E_{\max}}{\max\left\{\left|\frac{dI(t)}{dt}\right|\right\}} \frac{dI(t)}{dt}$$

which are specified by the lightning current *I(t)* and the peak magnetic and electric fields, B_{max} and E_{max}, respectively. I_{max} is the peak of the lightning current *I(t)*.

We assume that the sensitive components can be modeled using simple, canonical antennas such as monopoles and loops. In this report we consider only monopole antennas. The electric fields will be coupled into monopoles in the Faraday cage, and a voltage will be induced across the antenna terminals. The voltage induced across the antenna terminals can be modeled with a simple circuit model described in Section 6.0 and depicted in Figure 1. The magnitude of the open circuit antenna voltage is the product of the electric field and the effective height of the antenna, $h_{effective}$:

$$V_{OC}(t) = -E(t)\, h_{effective} \text{ where}$$

$$h_{effective} \approx \frac{h_{monopole}}{2} \quad ,$$

and the antenna capacitance C_A is

$$C_A = \frac{h}{60c\left[\ln\left(\frac{h}{a}\right) - 1\right]},$$

with *h* and *a* equal to the physical height and radius, respectively, of the monopole in meters.

The purpose of this report is to experimentally validate the circuit model in Figure 1. We use capacitance values from a variety of sources: the analytical formula above, numerical EM simulation, and measured values. For effective height we use values from the analytical formula above and numerical EM simulation.

First we validate capacitance values from the antenna capacitance formula and from numerical EM simulation. Then we validate the output of the circuit model in the time domain (with capacitance from the analytical formula, numerical EM simulation, and direct measurement and with $h_{effective}$ from the analytical formula and simulation) using a simulated low-current, lightning-like waveform.

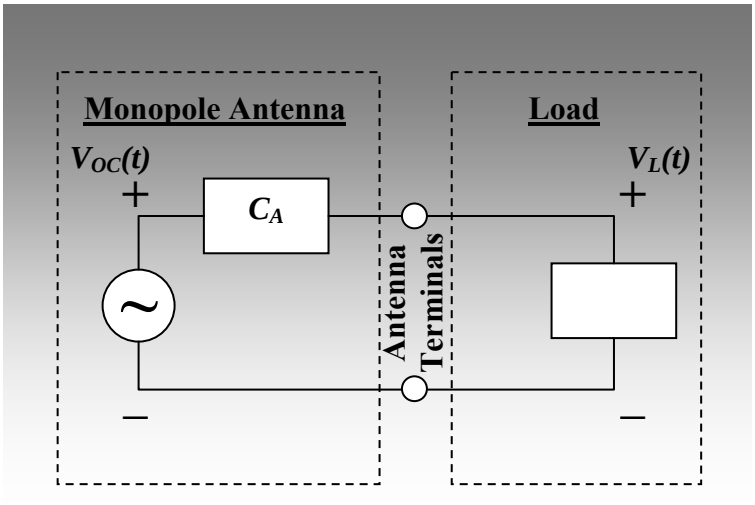

Figure 1: Simple monopole antenna circuit model from Section 6.0.

2.0 Experimental Validation

We made frequency-domain measurements to validate the capacitance values obtained from the analytical formula and simulation. We also made time-domain measurements to validate the circuit model, using capacitance values from the analytical formula, numerical EM simulation, and direct measurements and with $h_{effective}$ from the analytical formula and simulation. The primary components of the measurement setup are the two-meter high TEM cell; monopole antennas; and appropriate instrumentation for making frequency- and time-domain measurements. First we introduce the TEM cell, monopole antennas, and measurement instruments (network analyzer and oscilloscope). Then we describe the capacitance validation and time-domain validation of the circuit model.

2.1 Introduction

The LLNL TEM cell (Figure 2 and Figure 3) is a wave-guide-like device designed to maintain a 50Ω impedance while providing a workspace to study EM fields and their effects. This cell has one meter of vertical space between the inner conductor (septum) and the outer conductor (floor) and can be used for frequencies up to 90 MHz. The TEM cell creates nearly uniformly distributed fields in the one meter of vertical space between the septum and

the floor. The TEM (Transverse ElectroMagnetic) mode, where both the electric and magnetic fields are transverse to the direction of propagation and normal to each other, is the single mode produced in the cell below its cutoff frequency of 90 MHz. This cutoff frequency is considered high enough for the spectrum of interest in a lightning study.

Figure 3, the electric field is distributed vertically and the magnetic field surrounds the inner conductor with the magnetic flux lines appearing effectively parallel to the septum. The wave impedance from inner to outer conductor is 377Ω, the characteristic impedance of free space. The one-meter spacing gives the input voltage and electric field inside the cell a 1:1 relationship (in V/m).

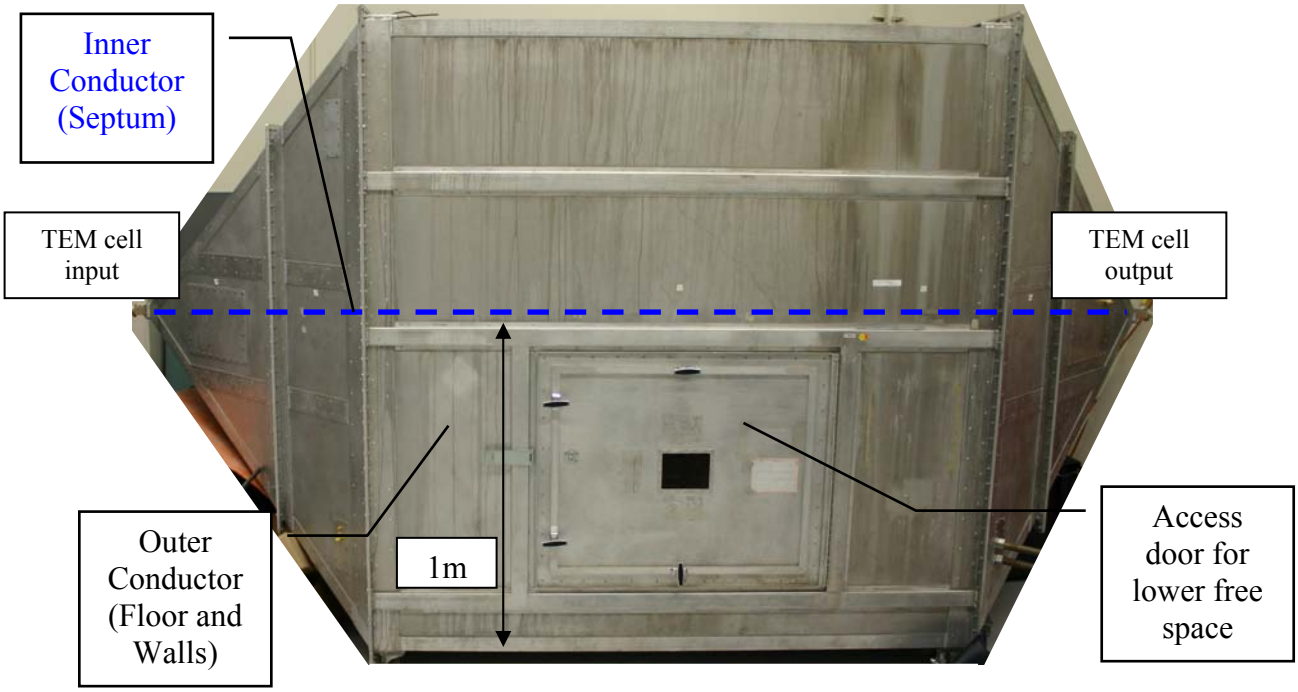

Figure 2: External view of two-meter TEM cell

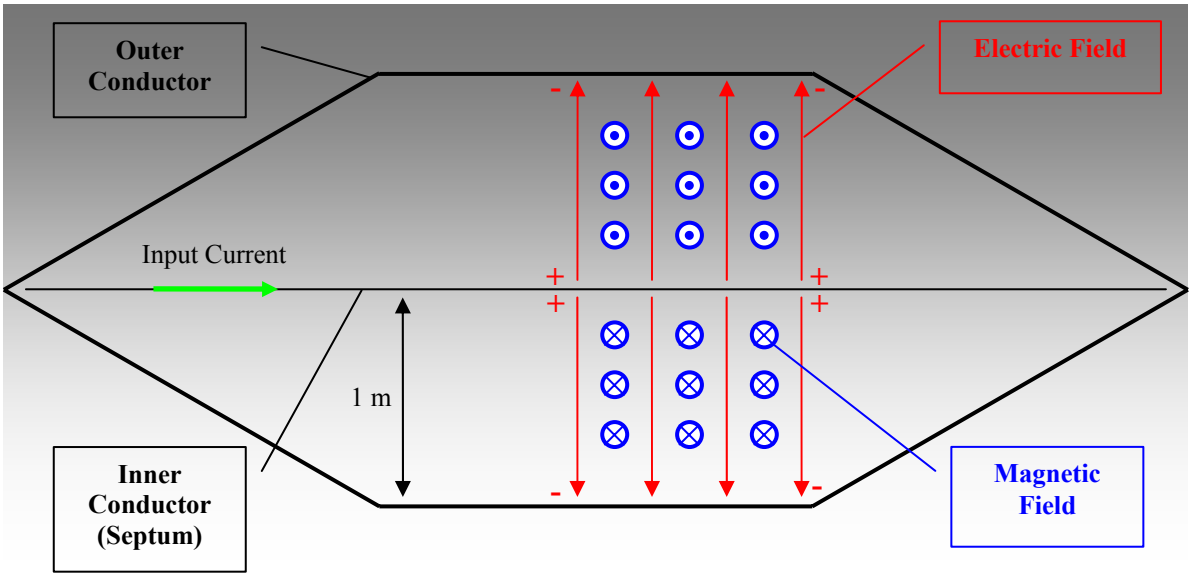

Figure 3: Fields in TEM cell---vertical cross section

We constructed a family of monopole antennas to study electric field coupling in the TEM cell. The monopoles vary in length from 1" (2.54 cm) to 6" (15.24 cm). We fabricated the monopoles from 0.141" outer diameter semi-rigid coaxial cable, also known as "Cujack". For each antenna, a length of outer conductor was removed, leaving the inner conductor and the Teflon insulator. The insulator provides additional structural support to the thin inner conductor. We also constructed a 0" monopole, which is a monopole with the inner conductor and Teflon insulator cut off at the end of the outer conductor. Figure 4 illustrates the monopole antennas. The antennas were attached to an elbow connector and affixed to the floor of the TEM cell using copper tape (Figure 5). The cable from the monopole to the network analyzer or oscilloscope passed through a non-isolated SMA feedthrough in the TEM cell wall.

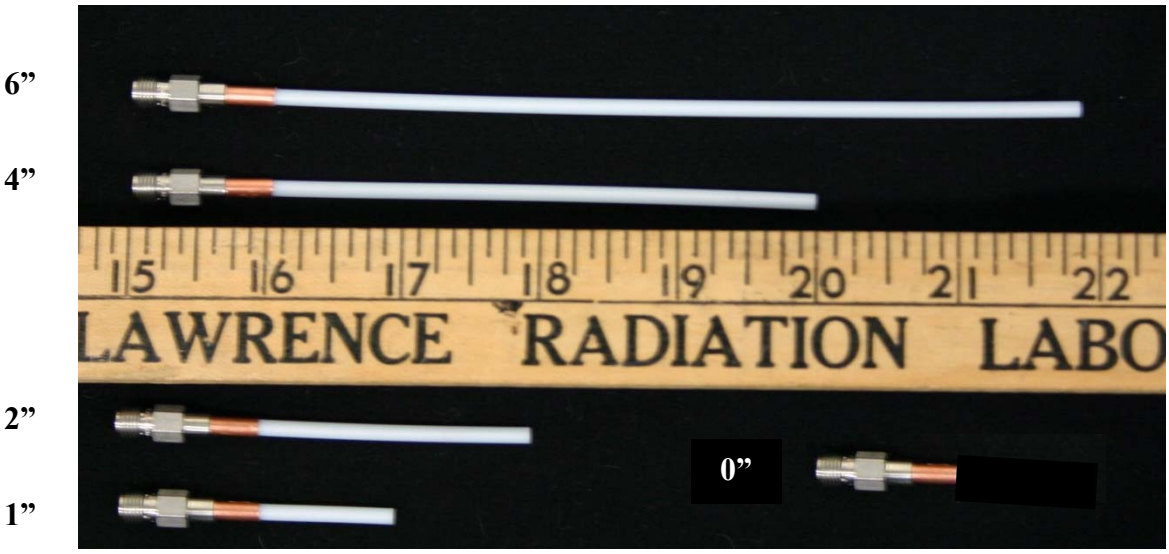

Figure 4: Monopole antennas

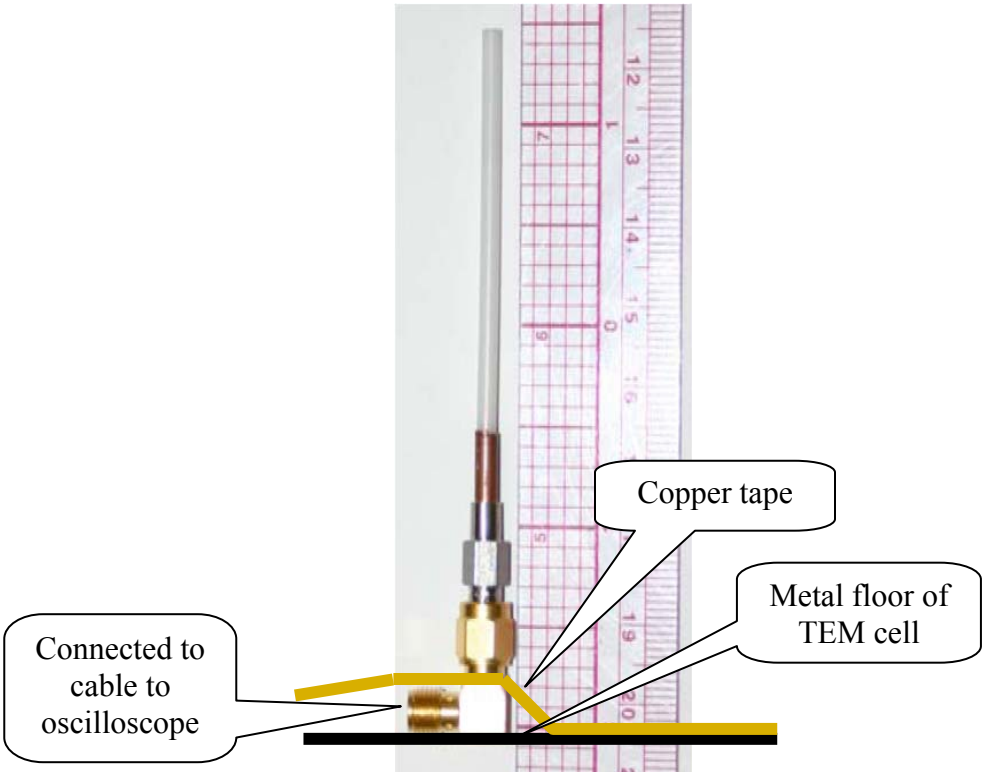

Figure 5: Monopole antenna attached to elbow connector and affixed to TEM cell floor using copper tape

In order to take measurements for validation, two primary instruments were employed. Frequency-domain measurements were made with an Agilent 4395A network analyzer. Time-domain measurements were made using a Tektronix 684C oscilloscope. In the case of the network analyzer, the instrument was connected to a laptop via GPIB for data collection. The data from the oscilloscope were recorded on floppies.

2.2 Capacitance Validation

We made measurements in the frequency domain using the network analyzer in the S_{11} (reflection) mode (Figure 6) in order to validate the analytical capacitance model and the capacitance values from numerical EM simulation. We calculate capacitance from S_{11} as follows:

$$C_L = \mathrm{Im}\left\{\frac{Y_L}{2\pi f}\right\}$$

with

$$Y_L = 1/Z_L \qquad Z_L = Z_0\left(\frac{1+S_{11}}{1-S_{11}}\right)$$

where f is frequency in Hertz, and Z_0 is the characteristic impedance of the transmission line in Ohms. The symbol C_L denotes the calculated "gross" capacitance value that includes an excess capacitance of 2.0 pF introduced by the coaxial portion of the antenna assembly, which is the 0" monopole portion---see Figure 4. Since this value is uniform across all antennas and is not a part of the antenna capacitance, it is subtracted from the gross capacitance measurements to obtain a measured value of the antenna capacitance. Figure 7 plots the gross capacitance values from the S_{11} data. When we subtract the excess coaxial capacitance from the gross capacitance measurements, the measured and predicted capacitance values agree to within 22% (22% for the shortest antenna and about 16% for the longer ones), with the predicted values lower than the measured values. See Table 1. The error is possibly due to the fact that the analytical formula is used somewhat outside of its region of validity, since the antenna is insulated and not a bare wire and there are perhaps fringing field effects near the termination of the outer conductor. If greater accuracy than the analytical formula is desired, then numerical EM simulations can be performed. EM simulations using Ansoft Maxwell yield capacitance values within 12% (12% for the shortest antenna and 4% to 7% for the longer ones). See Table 2.

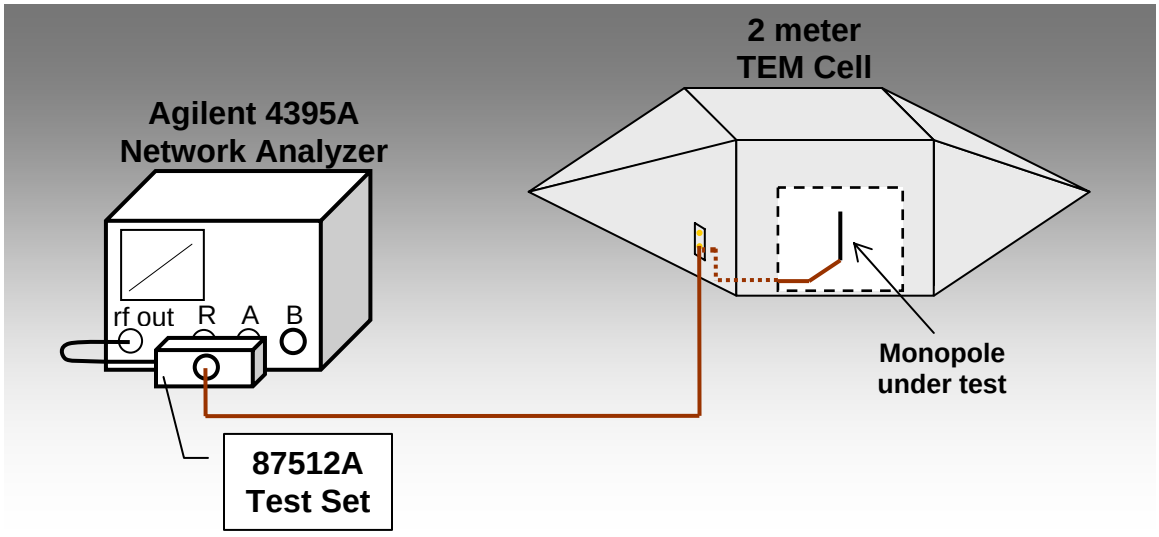

Figure 6: S_{11} Measurement to obtain reflection coefficient and capacitance

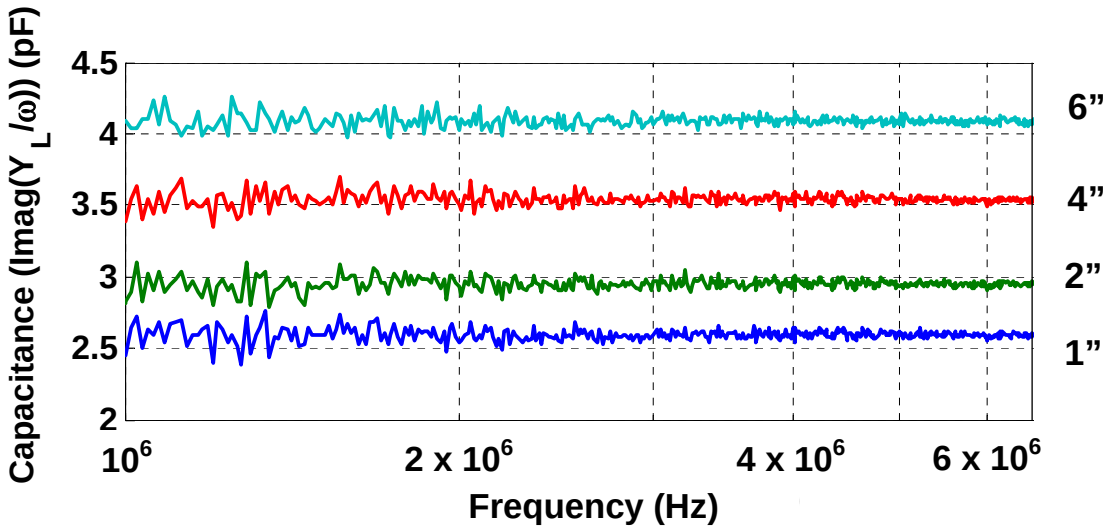

Figure 7: Gross capacitance values for monopole antennas

Table 1: Analytical capacitance formula predictions versus measured values

Antenna length	Predicted (pf)	Measured (pF)	Relative error
1”	0.47	0.6	-22%
2”	0.76	0.9	-16%
4”	1.28	1.5	-15%
6”	1.76	2.1	-16%

Table 2: Capacitance values from EM simulations versus measured values

Antenna length	Simulated (pf)	Measured (pF)	Relative error
1”	0.53	0.6	-12%
2”	0.86	0.9	-5%
4”	1.43	1.5	-4%
6”	1.96	2.1	-7%

2.3 Time-Domain Validation

Now we verify the complete circuit model for the case of a lightning-based excitation and low- and high-impedance load on the antenna and cable. We make measurements using an input waveform approximating the scaled first derivative of the lightning current and record the antenna output across 50Ω low-impedance and 1 MΩ – 10 pF high-impedance settings on the oscilloscope. The scaled first derivative of the lightning current is used because the electric field inside a hardened cell is approximately proportional to the first derivative of the input current during a strike. Refer to Figure 8 for the experimental setup. Figure 9 shows the electric field developed inside the TEM cell due to a typical input waveform. The rise time of this signal is about 200 ns and its duration is about 475 ns (full-

width half maximum). The magnitude of the field is limited by the maximum output of the waveform generator (+5 V).

For this report, in both the 50Ω low-impedance and 1 MΩ – 10 pF high-impedance cases we solve the circuit model for the output voltage using signal processing techniques in MATLAB [1]. We employ a digital filter to compute the output voltage given the input electric field strength (Figure 9). We also smooth the resulting output voltage with a moving-average filter. However, the circuit model can be solved using many other methods, such as implementing it in a circuit simulator.

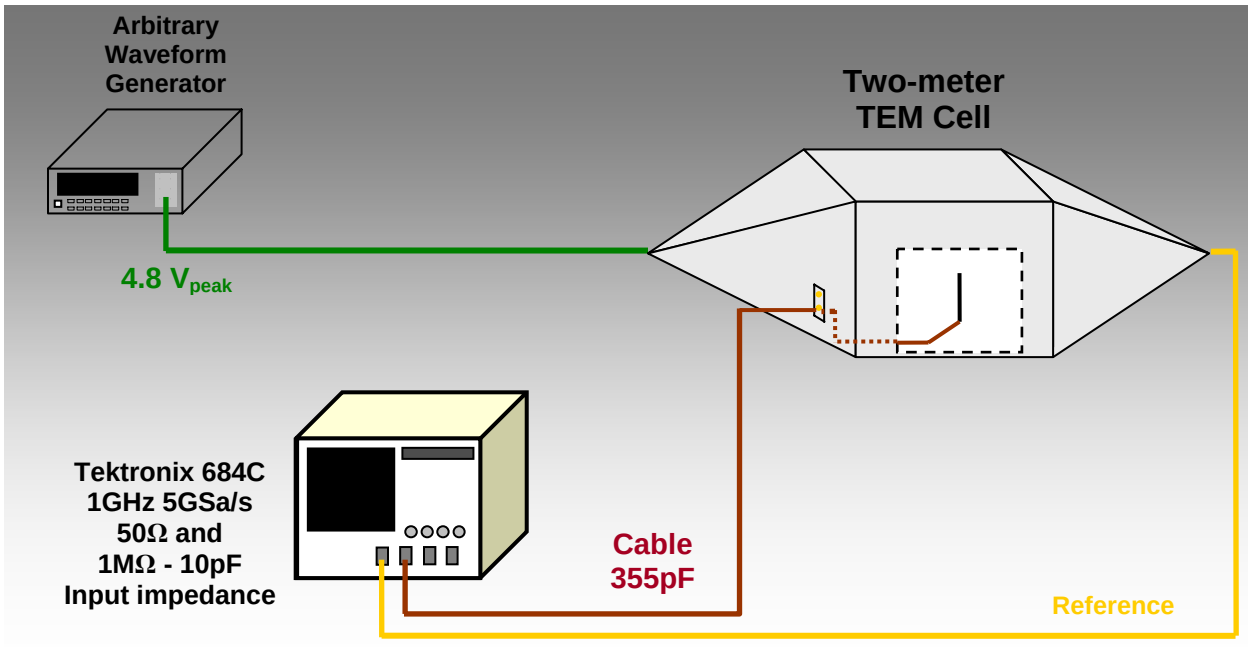

Figure 8: Experimental setup for time domain coupling measurements

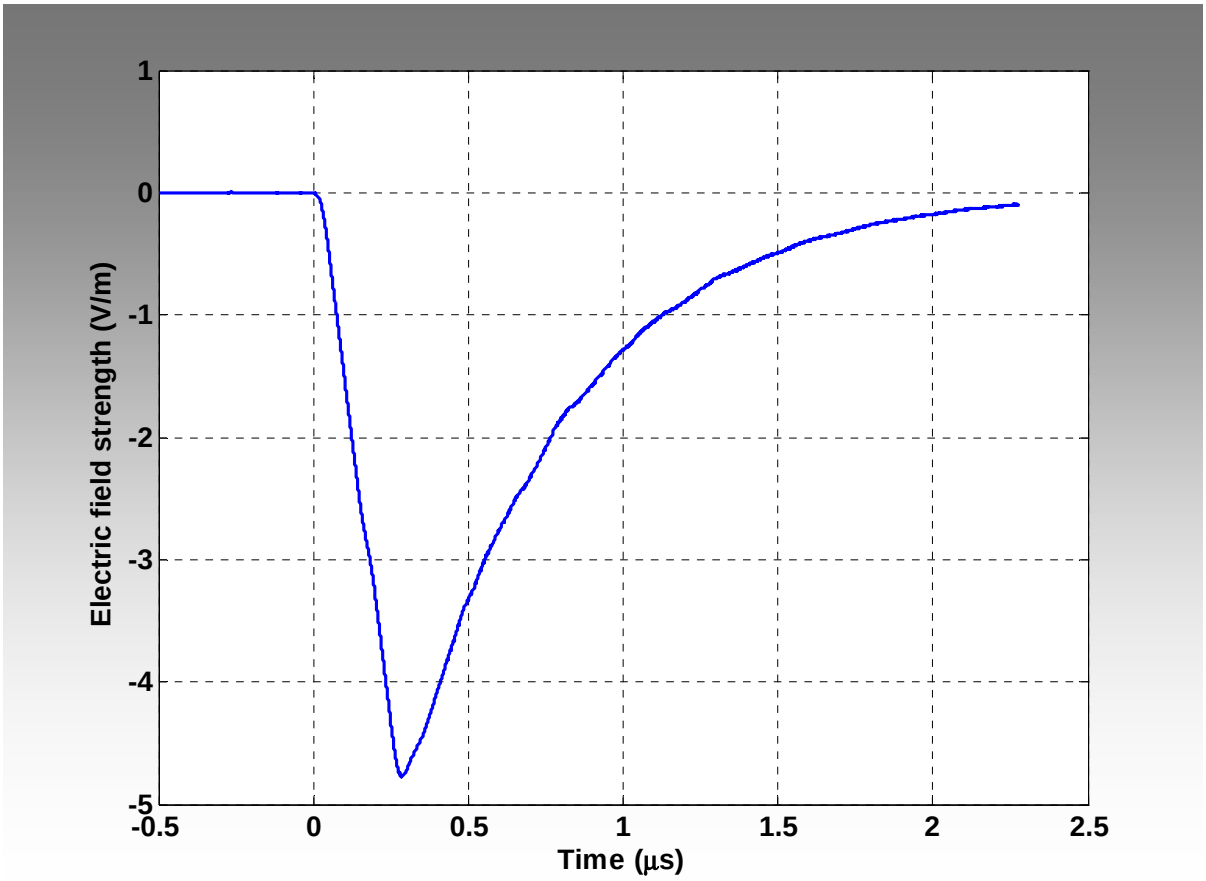

Figure 9: Electric field inside the TEM cell created by a typical input dI/dt profile waveform

2.3.1 Low-impedance (50Ω) scope load

First, we consider the antenna voltage output across the 50Ω low-impedance setting on the oscilloscope. The equivalent circuit model for the 6" monopole is depicted in Figure 10. The analytical formulas for the 6" monopole yield the modeled result for $V_L(t)$ shown in Figure 12. The measured trace is also plotted in Figure 12. The relative error in the maximum values is -21%, which could be due to using both the capacitance and effective height formulas outside of their regions of validity. Relevant comments on the capacitance formula have been made in the capacitance validation section (Section 2.2). The effective height formula is for a monopole directly over a ground plane, while in the time-domain measurement setup the monopole is elevated above the ground plane by about 1.5" (refer to Figure 5). This would tend to increase the real effective height so that the effective height formula would provide underestimates. Using simulated values from Ansoft Maxwell and HFSS for C_A and $h_{effective}$ yields much better results, which are very close to the measured values, as shown in Figure 13. If we use the simulated value for $h_{effective}$ and the measured value for C_A (see Table 1 and Table 2), then the relative error is 7%. Refer to Figure 14. The drop in the voltage around 0.17 μs is due to an inflection point in the input waveform (Figure 9). Filtering and smoothing edge effects for times before -0.5 μs are present but not shown in Figure 12, Figure 13, and Figure 14.

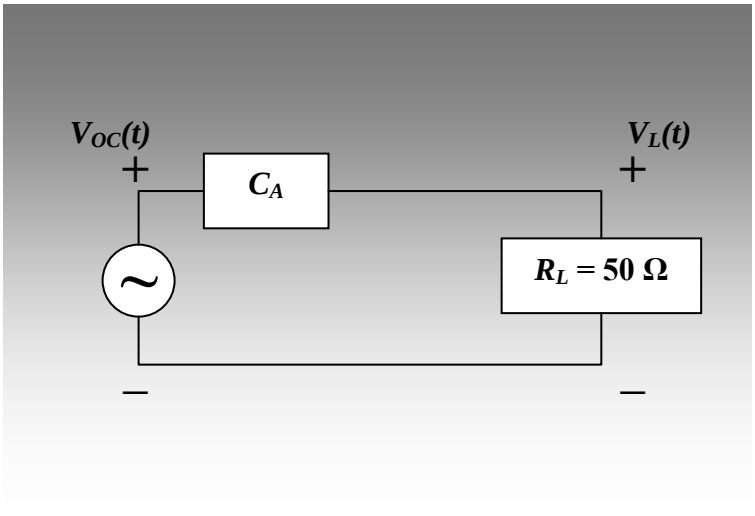

Figure 10: Equivalent circuit model for the 6" monopole with the 50Ω oscilloscope setting.

2.3.2 High-impedance (1 MΩ – 10 pF) scope load

Next, we consider the antenna voltage output across the 1 MΩ – 10 pF high-impedance setting on the oscilloscope. The equivalent circuit model for the 6" monopole is somewhat more complicated and is depicted in Figure 11. The capacitance C_{out} is the capacitance of the antenna output cable, running from the antenna, through the SMA feedthrough, to the oscilloscope (see Figure 8). C_{out} must be included because of the mismatch between the oscilloscope load and the antenna output cable characteristic impedance. The analytical formulas for the 6" monopole yield the modeled result for $V_L(t)$ shown in Figure 15. The measured trace is also plotted in Figure 15. The relative error in the maximum values is -32%, with the comments in Section 2.3.1 also applying here. Additionally, errors in the value of C_{out}, which in all of the cases in this section is an analytically-determined estimate (not measured), could cause some of the observed discrepancy. Again, using simulated values from Ansoft Maxwell and HFSS for C_A and $h_{effective}$ yields much better results, which have a relative error of -13% (Figure 16). If we use the simulated value for $h_{effective}$ and the measured value for C_A (see Table 1 and Table 2), then the relative error is -8%, as is depicted in Figure 17.

The relative errors for all of the low- and high-impedance cases are summarized in Table 3. The most accurate methods overall are using the measured value for the capacitance, with the effective height from EM simulation, followed by using the values from the EM simulation. However, using values from the analytical formulas still provides somewhat accurate results, even though the formulas are used outside of their regions of validity. We expect the results to improve as more accurate analytical formulas are employed.

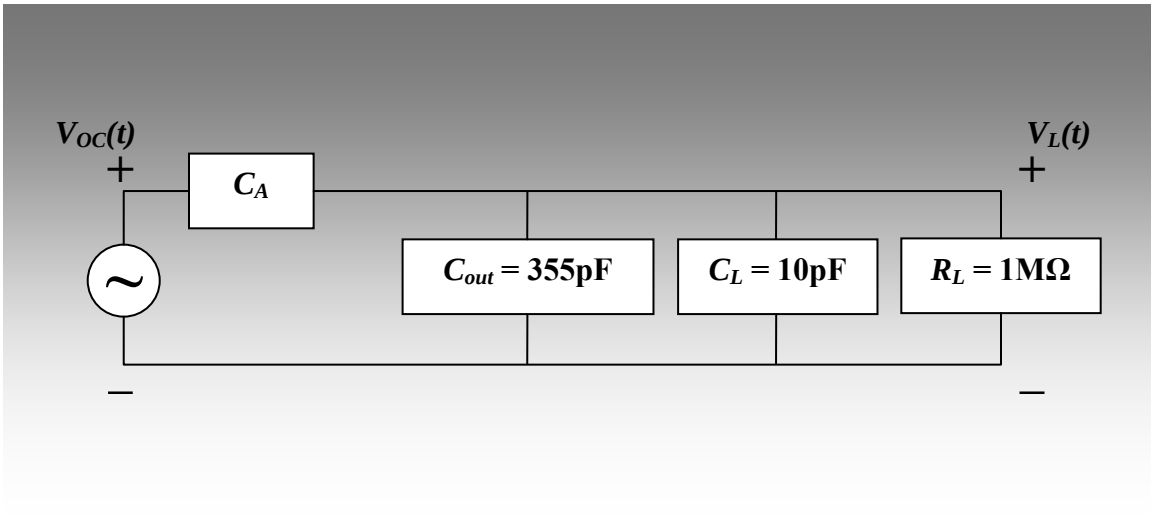

Figure 11: Equivalent circuit model for the 6" monopole with the 1MΩ – 10 pF oscilloscope setting.

Table 3: Relative errors for different methods of computing the antenna capacitance C_A and effective height $h_{effective}$

	C_A and $h_{effective}$ from analytical formulas	C_A and $h_{effective}$ from EM simulation	C_A from measurement, $h_{effective}$ from EM simulation
Low-impedance (50Ω)	-21%	~0%	7%
High-impedance (1 MΩ – 10 pF)	-32%	-13%	-8%

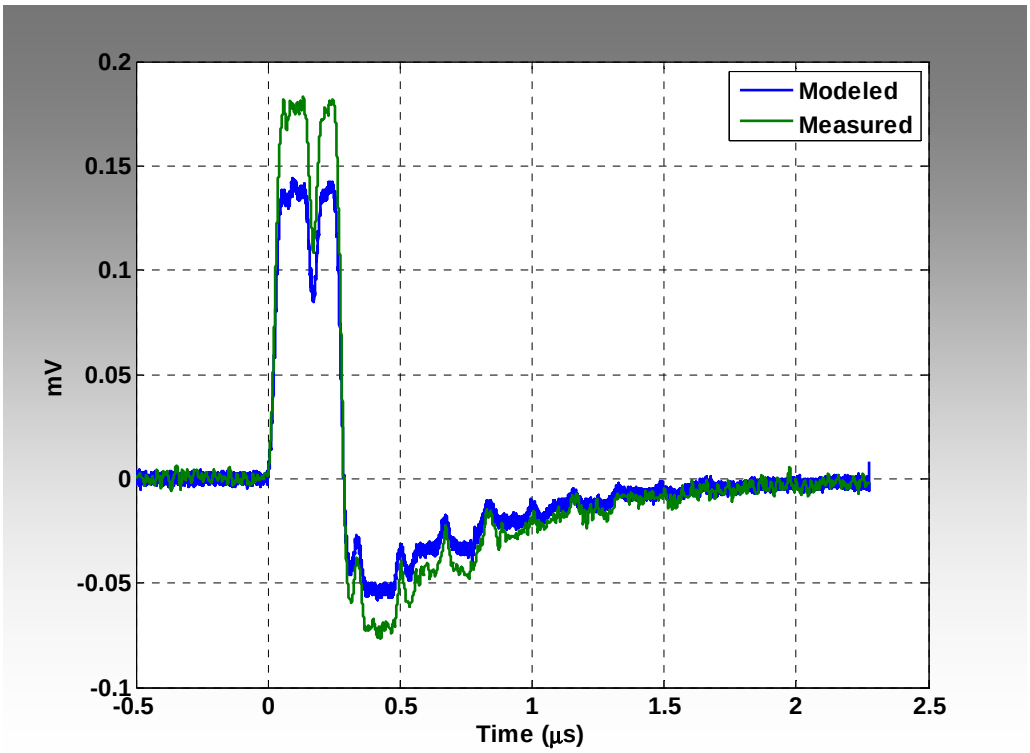

Figure 12: Low-impedance (50Ω) oscilloscope setting---modeled result using analytical formulas versus the measured trace for the 6" monopole (-21% relative error)

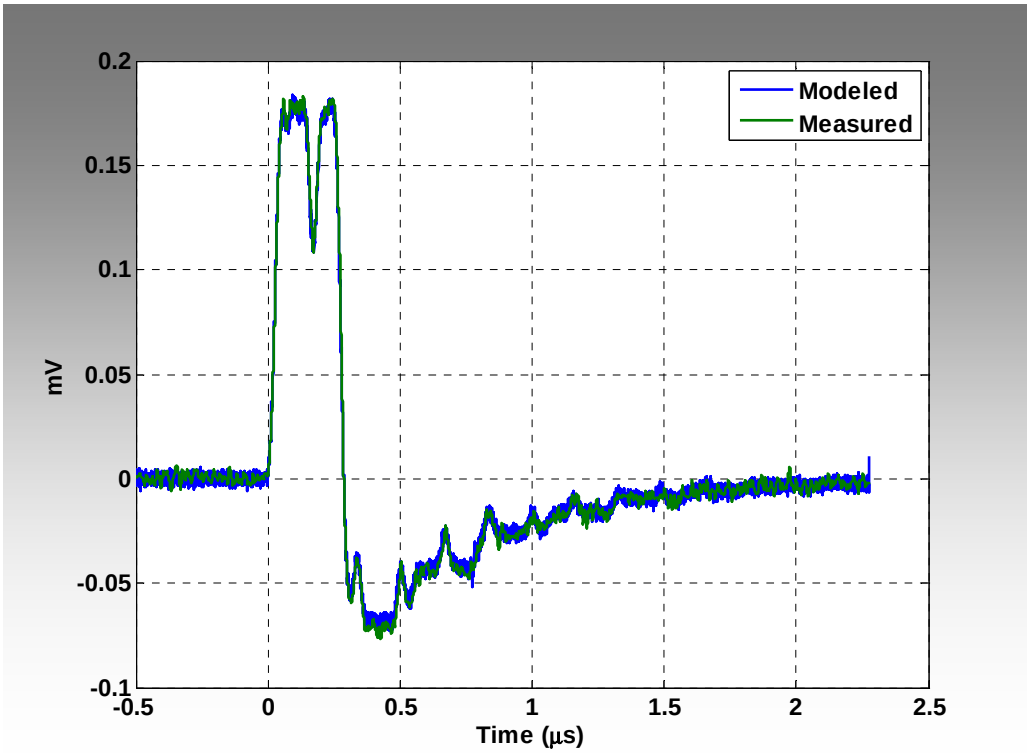

Figure 13: Low-impedance (50Ω) oscilloscope setting---modeled result using simulation values versus the measured trace for the 6" monopole (~0% relative error)

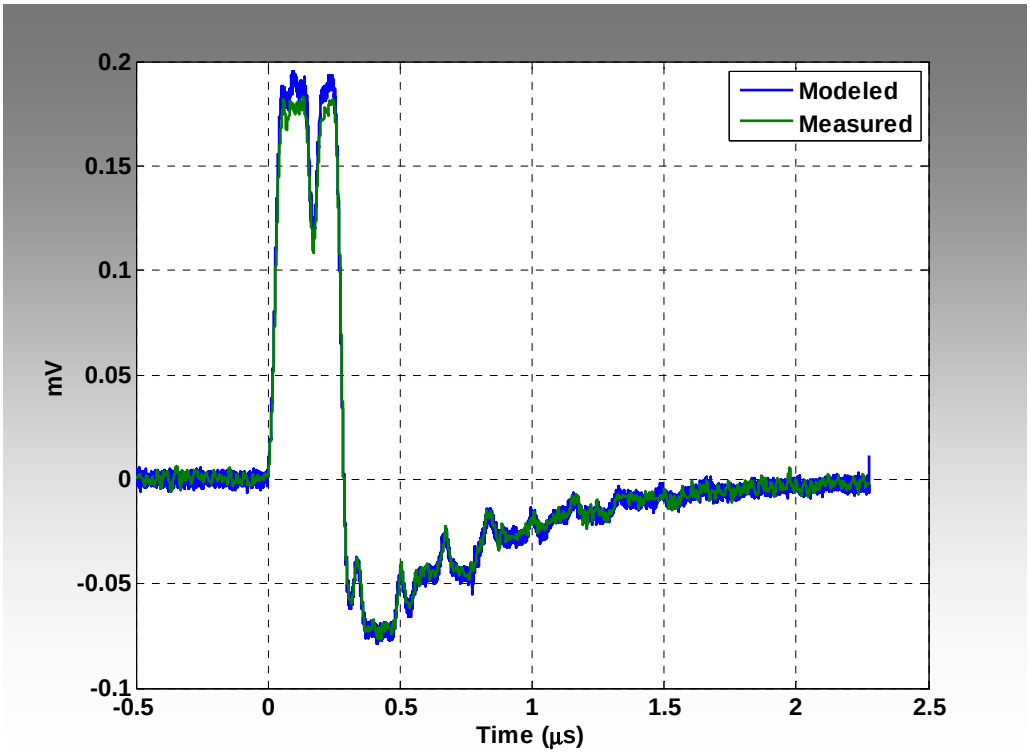

Figure 14: Low-impedance (50Ω) oscilloscope setting---modeled result, using measured capacitance value (see Table 1 and Table 2) and effective height from simulation, versus the measured trace for the 6" monopole (7% relative error)

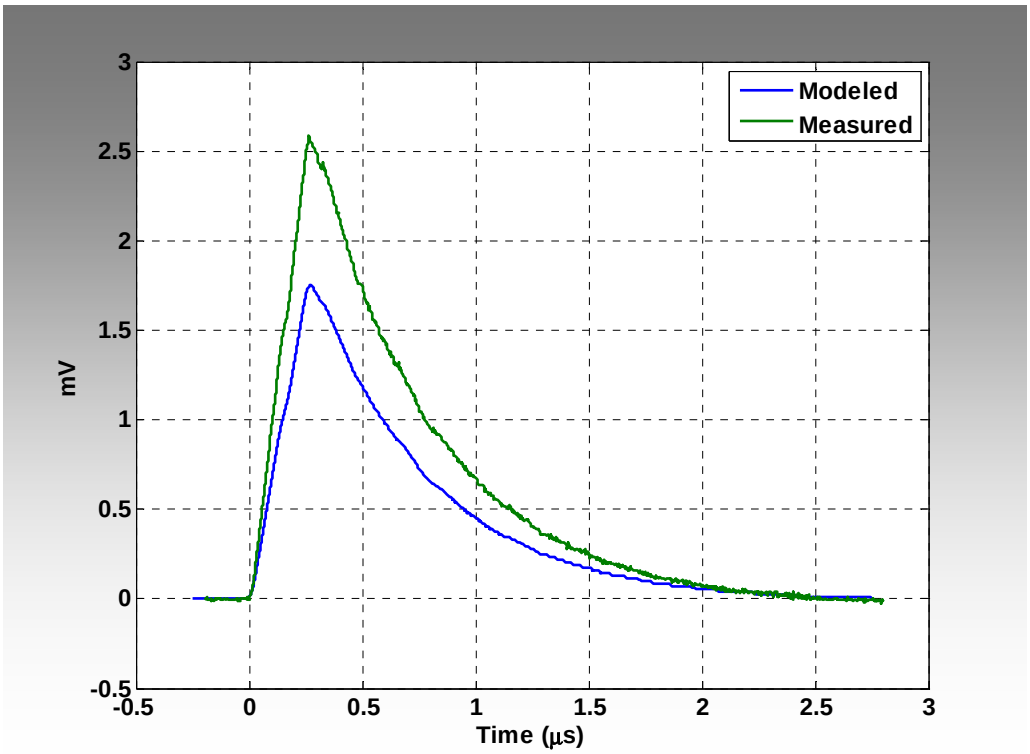

Figure 15: High-impedance (1 MΩ – 10 pF) oscilloscope setting---modeled result using analytical formulas versus the measured trace for the 6" monopole (-32% relative error)

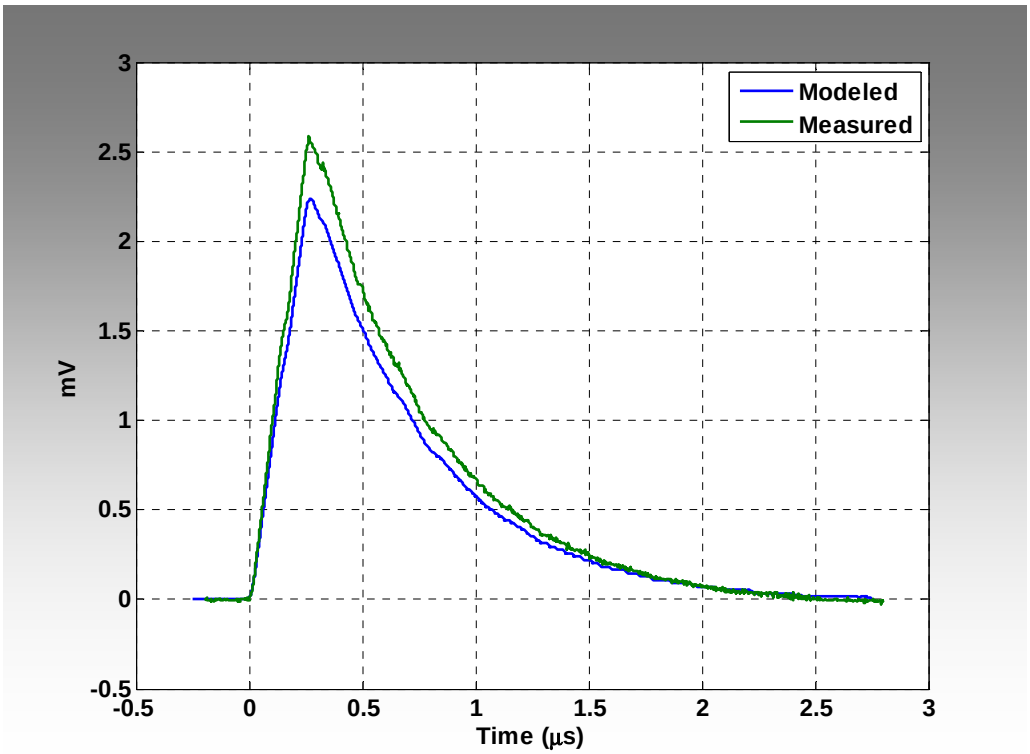

Figure 16: High-impedance (1 MΩ – 10 pF) oscilloscope setting---modeled result using simulation values versus the measured trace for the 6" monopole (-13% relative error)

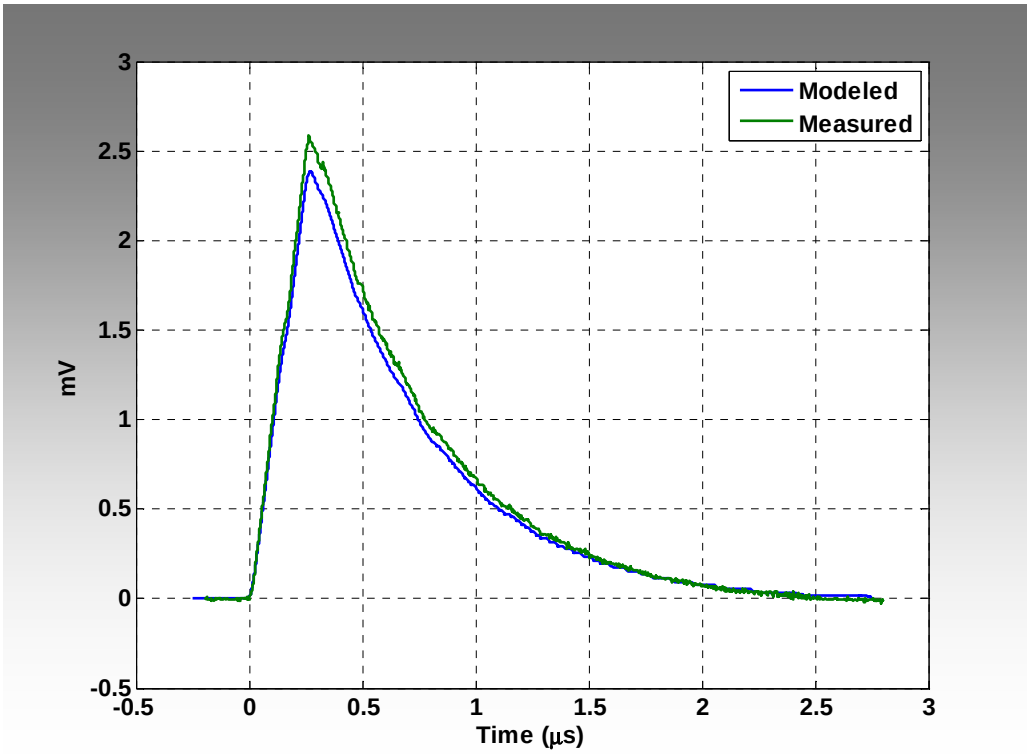

Figure 17: High-impedance (1 MΩ – 10 pF) oscilloscope setting---modeled result, using measured capacitance value (see Table 1 and Table 2) and effective height from simulation, versus the measured trace for the 6" monopole (-8% relative error)

2.4 Conclusions

For short monopoles in this low-power case, it has been shown that a simple circuit model is capable of accurate predictions for the shape and magnitude of the antenna response to lightning-generated electric field coupling effects, provided that the elements of the circuit model have accurate values. Numerical EM simulation can be used to provide more accurate values for the circuit elements than the simple analytical formulas, since the analytical formulas are used outside of their region of validity. However, even with the approximate analytical formulas the simple circuit model produces reasonable results, which would improve if more accurate analytical models were used.

2.5 Summary

This report discusses the coupling analysis approaches taken to understand the interaction between a time-varying EM field and a short monopole antenna, within the context of lightning safety for nuclear weapons at DOE facilities. It describes the validation of a simple circuit model using laboratory study in order to understand the indirect coupling of energy into a part, and the resulting voltage. Results show that in this low-power case, the circuit model predicts peak voltages within approximately 32% using circuit component values obtained from analytical formulas and about 13% using circuit component values obtained from numerical EM simulation. We note that the analytical formulas are used

outside of their region of validity. First, the antenna is insulated and not a bare wire and there are perhaps fringing field effects near the termination of the outer conductor that the formula does not take into account. Also, the effective height formula is for a monopole directly over a ground plane, while in the time-domain measurement setup the monopole is elevated above the ground plane by about 1.5" (refer to Figure 5).

3.0 Acknowledgements

We thank Mike Perkins for the excellent Ansoft Maxwell and HFSS simulations.

4.0 References

[1] ME Morris *et al.*, "Rocket-triggered lightning studies for the protection of critical assets," *IEEE Transactions on Industry Applications*, vol. 30, no. 3, May-June 1994, pp. 791-804.

[2] The MathWorks MATLAB R2007b.

5.0 Appendix A---Introductory and background material

When lightning strikes a steel-reinforced concrete building, electromagnetic (EM) fields are generated inside the building. When the building is hardened into a "Faraday cage", it is still not a perfect shield, due to apertures and imperfect conductors, and there will be EM fields inside. Intact nuclear weapon systems are not vulnerable to EM fields because they are hardened to withstand the DOE Stockpile-to-Target Sequence (STS) [2] lightning threat. However, this situation is very different for a nuclear weapon being disassembled or assembled. Any wires attached to internal components, such as detonators, will extract RF energy from the fields. Therefore, lightning is a possible threat to exposed weapons, so safety assessments are required.

Figure 18 shows the overall safety assessment process. The bottom half of the figure depicts the process to determine the frequency of lightning strikes, which are also known as "flashes". The inputs include the flash density, the facility size, and the duration of the critical operations. If the strike frequency, usually specified as flashes per year, is sufficiently low, then the component vulnerability does not have to be computed. This is rarely the case for high-consequence accidents, like detonating a nuclear weapon.

The vulnerability analysis assumes a lightning strike that creates a stress, e.g., voltage, on a critical component. The strength of the component is compared against the stress, and if the strength is much greater, then the component is safe. For example, if a lightning strike generates 10 volts on a detonator and the detonator requires 1,000 volts to initiate, the safety margin is large, and the vulnerability is extremely low. In reality there will be many different levels of stresses and strengths, and the vulnerability should be expressed as a probability. See Figure 19. When vulnerability is combined with the frequency of a strike, the chance of an accidental detonation is even lower. If likelihood of an accident is not sufficiently low, safety controls are required.

The strength levels are usually determined experimentally, and each component will have a mean strength with some variation. The stress levels are determined by EM environment variables (rise rates of the lightning current, attachment point, and the quality of the Faraday cages) and coupling issues (location, length, and orientation of the component wires). Estimating the stress levels is a complex and crucial step in the risk assessment, which is challenging for three reasons:

- The fields inside the facilities with complex geometries are difficult to compute.
- The energy in the fields is spread over a broad frequency spectrum from almost direct-current (DC) to megahertz (MHz), since the lightning current is an impulse.
- The exposed wires are non-traditional antennas that operate in the near-field rather than the usual far-field. While the traditional antenna designs match the physical size to the operating wavelength, the weapon "antennas" are relatively short when compared with the wavelength of the EM pulse.

However, these challenges are manageable. We meet these challenges by using simple circuit models, validated experimentally, to estimate the coupled voltages and energies. The

experimental validation is necessary because of the importance and complexity of the problem.

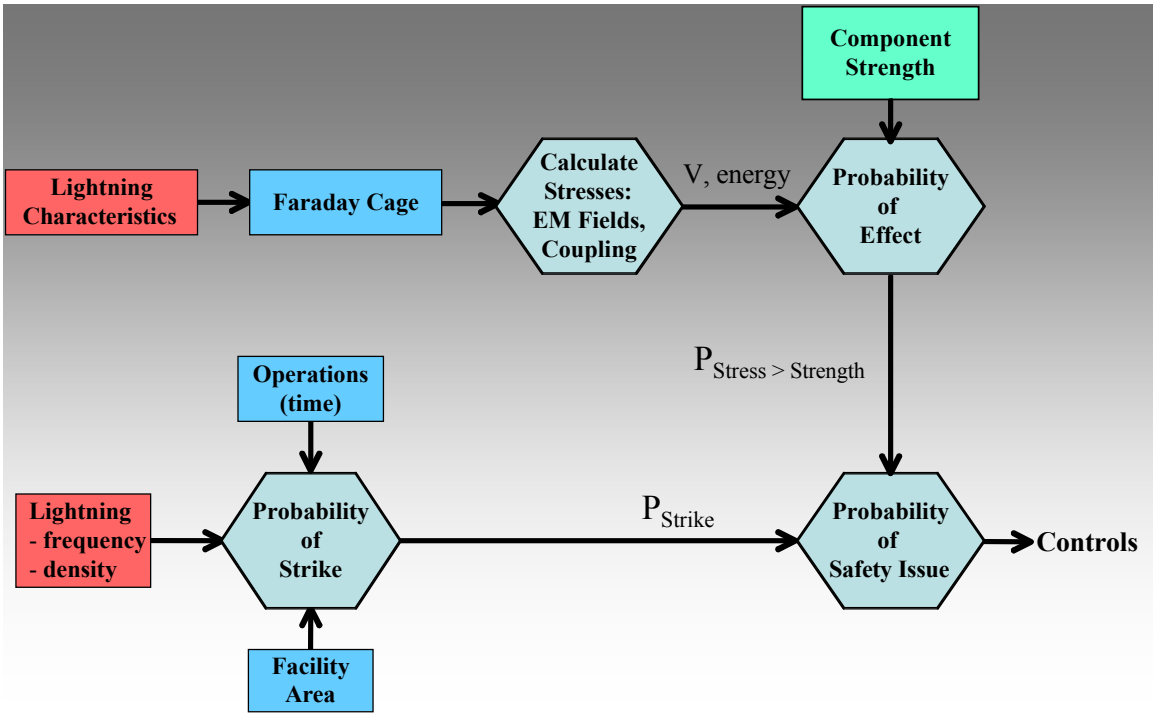

Figure 18: The probability of an accident depends on the frequency of a lightning strike and the vulnerability of components.

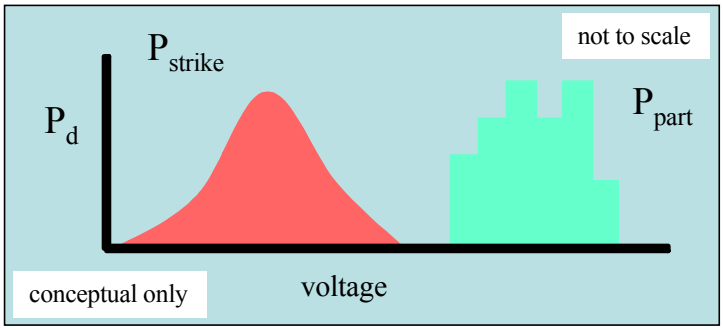

Figure 19: Stress (P_{strike}) and strength (P_{parts}) levels can be specified with probability density distributions, P_d.

5.1 References

[1] RJ Fisher and MA Uman, "Recommended Baseline Direct-Strike Lightning Environment for Stockpile-to-Target Sequences", Sandia Report SAND89-0192, May 1989.

6.0 Appendix B---Calculation of the Load Voltage of Short Monopole Antennas

6.1 Circuit model

The load voltage of a monopole antenna over a ground plane in the frequency domain is [1]

$$V_L(f) = \frac{V_{OC}(f) Z_L(f)}{Z_A(f) + Z_L(f)} = \underbrace{-h_e(f) E^{inc}(f)}_{V_{OC}(f)} \underbrace{\frac{Z_L(f)}{Z_A(f) + Z_L(f)}}_{\text{Voltage divider}}, \quad (1)$$

where V_{OC} is the open circuit voltage of the monopole; h_e is the effective height; E^{inc} is the incident electric field parallel to the monopole (positive if E^{inc} is oriented in the direction from the ground plane to the end of the monopole); Z_A is the antenna input impedance; and Z_L is the load impedance. Refer to Figure 20 for the frequency-domain circuit model of Eqn. (1). Note that $V_{OC}(f) = -h_e(f)\, E^{inc}(f)$ in Figure 20.

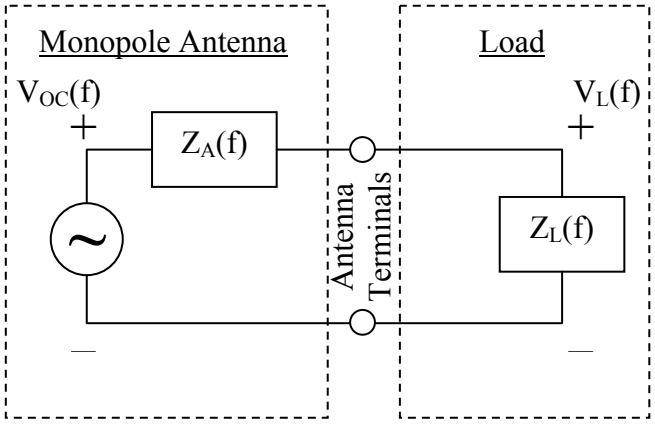

Figure 20: Frequency-domain circuit model of the load voltage of a short monopole antenna

The input impedance of a short monopole is dominated by capacitance and can be approximated as [2]

$$Z_A(f) = \frac{1}{j2\pi f C}$$
$$C = \frac{h}{60c\left[\ln\left(\frac{h}{a}\right) - 1\right]} \quad (2)$$

where c is the speed of light in free space, and a is the radius of the monopole antenna. (If we define h as the physical height of a monopole antenna, then the antenna can be considered "short" [1] if $2\pi h / \lambda << 1$, where λ is the minimum wavelength of interest). The effective height of a short monopole is a function of its physical height [1]:

$$h_e(f) = \frac{h(\Omega - 1)}{2(\Omega - 2 + \ln 4)} \quad \left(\approx \frac{h}{2} \text{ for } \Omega \geq 7 \right)$$
$$\Omega \equiv 2\ln\left(2h/a\right) \tag{3}$$

The symbol Ω here is referred to as the "fatness parameter". According to [1], Ω must be greater than or equal to 7, "since the present theory of cylindrical antennas is not valid for smaller values of Ω". See Figure 21.

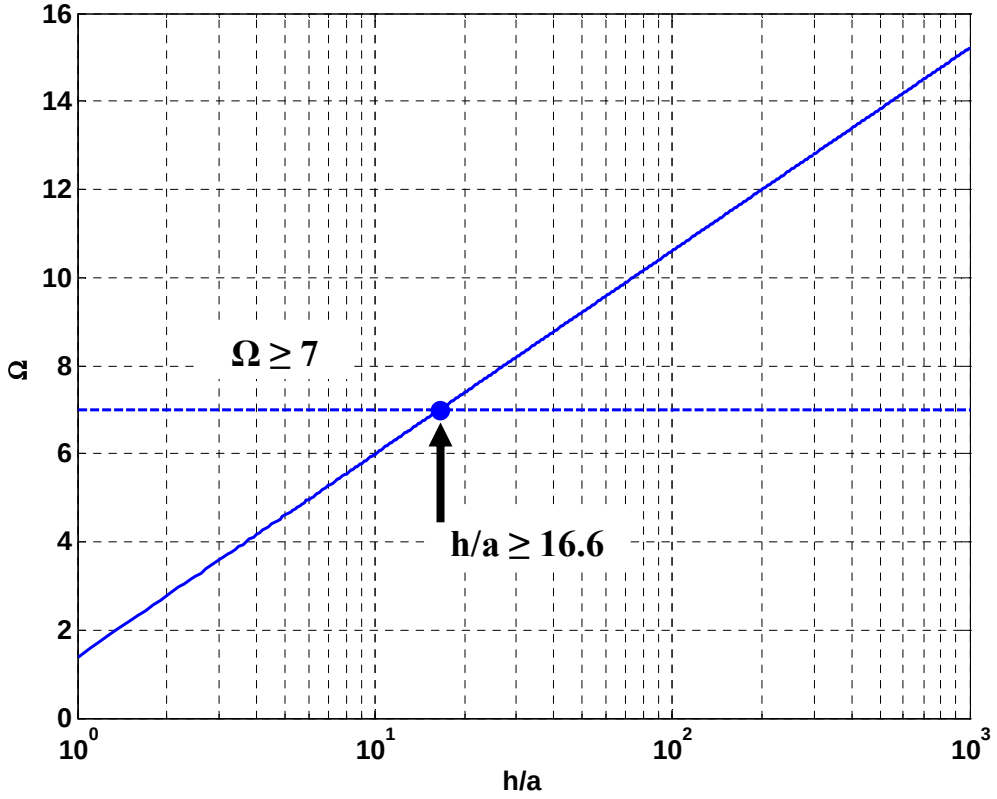

Figure 21: Fatness parameter Ω versus h/a. Ω must be greater than or equal to 7 for the theory in this report to hold [1].

Equation (1) in the Laplace domain, using the approximation in (3), is

$$V_L(s) = -\frac{h}{2} E^{inc}(s) \frac{Z_L(s)}{Z_A(s) + Z_L(s)} \tag{4}$$

The inverse Laplace transform yields the time-domain equivalent:

$$\boxed{V_L(t) = -\frac{h}{2} E^{inc}(t) * L^{-1}\left\{ \frac{Z_L(s)}{Z_A(s) + Z_L(s)} \right\}} \tag{5}$$

where $E^{inc}(t)$ is the inverse Laplace transform of $E^{inc}(s)$. The symbol "L^{-1}" represents the inverse Laplace transform. The "*" symbol denotes convolution.

6.2 Special cases

$|\mathbf{Z_L}| >> |\mathbf{Z_A}|$

If $|Z_L| >> |Z_A|$, we can simplify (1) as follows. Let

$$\alpha = {Z_A(f)}\Big/{Z_L(f)} \tag{6}$$

then

$$V_L(f) = -\frac{h}{2}E^{inc}(f)\frac{1}{1+\alpha} = -\frac{h}{2}E^{inc}(f)\{1+O(\alpha)\} \approx -\frac{h}{2}E^{inc}(f) \tag{7}$$

which is

$$V_L(s) \approx -\frac{h}{2}E^{inc}(s) \tag{8}$$

in the Laplace domain. The inverse Laplace transform yields the time-domain equivalent:

$$\boxed{V_L(t) \approx -\frac{h}{2}E^{inc}(t)} \tag{9}$$

where $E^{inc}(t)$ is the inverse Laplace transform of $E^{inc}(s)$.

$|\mathbf{Z_L}| << |\mathbf{Z_A}|$

If $|Z_L| << |Z_A|$, we can simplify (1) as follows [1]. Let

$$\alpha = {Z_L(f)}\Big/{Z_A(f)} \tag{10}$$

then

$$V_L(f) = -\frac{h}{2}E^{inc}(f)\frac{\alpha}{1+\alpha} = -\frac{h}{2}E^{inc}(f)\{\alpha+O(\alpha^2)\} \approx -\frac{h}{2}E^{inc}(f)\frac{Z_L(f)}{Z_A(f)} \tag{11}$$

Using (2) we have

$$V_L(f) \approx -j2\pi f\frac{h}{2}CE^{inc}(f)Z_L(f) \tag{12}$$

which is

$$V_L(s) \approx -s\frac{h}{2}CE^{inc}(s)Z_L(s) \tag{13}$$

in the Laplace domain. The inverse Laplace transform yields the time-domain equivalent:

$$\boxed{V_L(t) \approx -C\frac{h}{2}\left[\frac{dE^{inc}(t)}{dt} * Z_L(t)\right]} \tag{14}$$

where $E^{inc}(t)$ and $Z_L(t)$ are the inverse Laplace transforms of $E^{inc}(s)$ and $Z_L(s)$, respectively.

$Z_L = R_L$

If $Z_L = R_L$, then in the Laplace domain, using (1) and (2),

$$V_L(s) = -\frac{h}{2} E^{inc}(s) \frac{R_L}{1/sC + R_L} \tag{15}$$

Since

$$\frac{R_L}{1/sC + R_L} = \frac{sR_L C}{1 + sR_L C} = \frac{s}{s + 1/R_L C} \tag{16}$$

we have

$$V_L(s) = -\frac{h}{2} sE^{inc}(s) \frac{1}{s + 1/R_L C} \tag{17}$$

and the inverse Laplace transform yields

$$\boxed{V_L(t) = -\frac{h}{2}\left[\frac{dE^{inc}(t)}{dt} * e^{-t/\tau} u(t)\right]} \tag{18}$$

where $\tau = R_L C$, and u(t) denotes the unit step function. Thus, $V_L(t)$ is proportional to a low-pass filtered version of $dE^{inc}(t)/dt$. Note that if $R_L >> |Z_A|$, we have

$$\boxed{V_L(t) \approx -\frac{h}{2} E^{inc}(t)} \tag{19}$$

since convolution by $e^{-t/\tau} u(t)$ for large τ is approximately equal to convolution by the step function, which approximates integration of $dE^{inc}(t)/dt$. Also note that if $R_L << |Z_A|$, we have

$$\boxed{V_L(t) \approx -R_L C \frac{h}{2} \frac{dE^{inc}(t)}{dt}} \tag{20}$$

since convolution by $e^{-t/\tau} u(t)$ for small τ is approximately equal to convolution by a scaled delta function.

$Z_L = R_L$ in parallel with C_L

If $Z_L = R_L$ in parallel with C_L, then in the Laplace domain, using (1) and (2),

$$V_L(s) = -\frac{h}{2} E^{inc}(s) \frac{sR_L C}{sR_L(C + C_L) + 1} = -\frac{h}{2} sE^{inc}(s) \frac{R_L C}{sR_L(C + C_L) + 1} \tag{21}$$

and the inverse Laplace transform yields

$$\boxed{V_L(t) = -\frac{h}{2}\left(\frac{C}{C + C_L}\right)\left[\frac{dE^{inc}(t)}{dt} * e^{-t/\tau} u(t)\right]} \tag{22}$$

with $\tau = R_L(C + C_L)$.

Table 4: Special cases

$$V_L(t) = -\frac{h}{2} E^{inc}(t) * L^{-1}\left\{\frac{Z_L(s)}{Z_A(s)+Z_L(s)}\right\}$$

$\|\mathbf{Z_L}\| >> \|\mathbf{Z_A}\|$	$V_L(t) \approx -\frac{h}{2} E^{inc}(t)$
$\|\mathbf{Z_L}\| << \|\mathbf{Z_A}\|$	$V_L(t) \approx -C\frac{h}{2}\left[\frac{dE^{inc}(t)}{dt} * Z_L(t)\right]$
$\mathbf{Z_L} = \mathbf{R_L}$	$V_L(t) = -\frac{h}{2}\left[\frac{dE^{inc}(t)}{dt} * e^{-t/\tau}u(t)\right], \tau = R_L C$
$\mathbf{R_L} >> \|\mathbf{Z_A}\|$	$V_L(t) \approx -\frac{h}{2} E^{inc}(t)$
$\mathbf{R_L} << \|\mathbf{Z_A}\|$	$V_L(t) \approx -R_L C\frac{h}{2}\frac{dE^{inc}(t)}{dt}$
$\mathbf{Z_L} = \mathbf{R_L}$ **in parallel with** $\mathbf{C_L}$	$V_L(t) = -\frac{h}{2}\left(\frac{C}{C+C_L}\right)\left[\frac{dE^{inc}(t)}{dt} * e^{-t/\tau}u(t)\right], \tau = R_L(C+C_L)$

6.3 References

[1] HJ Schmitt *et al*., "Calculated and Experimental Response of Thin Cylindrical Antennas to Pulse Excitation," *IEEE Transactions on Antennas and Propagation*, Vol. 14, No. 2, March, 1966, pp. 120-127.

[2] WL Stutzman and GA Thiele, *Antenna Theory and Design*, John Wiley & Sons, Inc., 1998, pp. 47 and 66.